Diffusion Tensor and Velocity Encoded Imaging for Fiber and Aponeurosis Strain Mapping of the Medial Gastrocnemius at Submaximal Isometric Contractions at Different Ankle Angles.

Journal:	*Journal of Magnetic Resonance Imaging*
Manuscript ID	Draft
Wiley - Manuscript type:	Research Article
Classification:	Physiological research applications < Imaging Principles and Education < Basic Science, Functional musculoskeletal imaging < Musculoskeletal imaging < Clinical Science, Muscle and skin < Musculoskeletal imaging < Clinical Science
Manuscript Keywords:	Velocity encoded phase contrast imaging, muscle fiber tracking, muscle fiber and aponeurosis strain mapping, ankle angle positions, muscle force-length curve
Note: The following files were submitted by the author for peer review, but cannot be converted to PDF. You must view these files (e.g. movies) online.	
Supporting Figure 1.gif Supporting Figure 2.gif	

Diffusion Tensor and Velocity Encoded Imaging for Fiber and Aponeurosis Strain Mapping of the Medial Gastrocnemius at Submaximal Isometric Contractions at Different Ankle Angles

ABSTRACT

Background: Muscle fiber architecture influences force production; study of structure-function relationship *in-vivo* will increase understanding of muscle physiology.

Purpose: To examine relationships of Medial Gastrocnemius (MG) muscle fiber and aponeurosis strains to muscle force at three-ankle angles (dorsiflexion: ***D***, neutral: ***N***, and plantar flexion: ***P***) in isometric contractions at 25% and 50%MVC combined with diffusion tensor imaging to extract fiber orientation.

Study Type: Prospective cohort study.

Subjects: 6 male subjects (33.2 ± 16.3 yrs.)

Field Strength/Sequence: 1.5T, Velocity encoded phase contrast and SE-EPI DTI.

Assessment: Fiber and aponeurosis strain, normalized strain (to force and torque), fiber length and pennation angle at rest and peak contraction analyzed for statistical differences between ankle positions, %MVC and fiber location.

Statistical Tests: Two-way repeated measures ANOVA and post hoc Bonferroni-adjusted tests for normal data. Related samples test with Friedman's 2-way ANOVA by ranks with corrections for multiple comparisons for non-normal data. All tests set $\alpha = 0.05$.

Results: DTI data was successfully utilized to extract muscle fibers. Significant differences were found in fiber length D-P ($p < 0.001$), D-N ($p = 0.023$) at rest and at peak contraction D-P ($p < 0.001$) and D-N ($p < 0.001$) and pennation angle D-P ($p = 0.029$) at rest and peak

contraction D-N ($p = 0.029$) and D-P ($p < 0.001$). Peak strain was significantly reduced at 25 %MVC ($p = 0.002$). Normalized strain revealed significant differences between ankle angles at both force levels and was significantly higher at 25 %MVC in the P position ($p = 0.029$). Muscle force and fiber length at each ankle angle was used to track the location on the Force-Length curve and showed the MG operates on the curve's ascending limb.

Data Conclusion: The dorsiflexed position generated significantly higher force with lower fiber strain than neutral and plantarflexed ankle positions.

Keywords: Velocity encoded phase contrast imaging, muscle fiber tracking, muscle fiber and aponeurosis strain mapping, ankle angle positions, muscle force-length curve

INTRODUCTION

Dynamic studies of isometric and plantarflexion contraction in skeletal muscle using cine-MRI or velocity-encoded phase contrast (VE-PC) MRI have revealed several aspects of muscle deformation that require further exploration (1-4). The muscle force-length (FL) relationship is well established and describes the dependence of the steady-state isometric force of a muscle (fiber, or sarcomere) as a function of muscle (fiber, sarcomere) length and it has been explained by the 'sliding filament' theory (5-7). In this theory, the maximal isometric force of a sarcomere is determined by the amount of overlap between the contractile filaments, actin, and myosin (6). At short lengths, force increases as sarcomere length increases (ascending slope), reaches a plateau at intermediate lengths (optimal length for maximum force production), followed by a decrease in force as sarcomere length increases (descending slope) at long muscle lengths. Muscle fiber architecture (fiber length and pennation angle) clearly influences force production. A study of this structure-function relationship *in-vivo* will reveal aspects of force production that can be used to understand muscle physiology in normal and in diseased states and to develop optimal exercise paradigms for rehabilitation or to maximize athletic performance (8-10). The triceps surae (TS) force-length relationship can be altered by changing the knee joint position, ankle joint position, or both. Several groups have examined the force produced by the TS plantar flexors (Soleus, Medial Gastrocnemius (MG), and Lateral Gastrocnemius (LG)) during isometric plantarflexion contraction for combinations of knee flexion and ankle positions (11-14). Prior studies have used electromyography (EMG) and ultrasound (US) to study muscle isometric plantarflexion force, activation, and muscle fiber architecture changes in the MG for combinations of knee flexion and ankle angles (11-14). These studies showed that while there were significant differences in fascicle length of the MG at rest for the different knee/ankle positions, these differences in length were not

seen at a maximal isometric plantar flexion contraction and the EMG activity of the biarticular MG during the MVC decreased at a pronounced flexed knee-joint position despite the fact there were no differences in MG fascicle length at maximum plantarflexion contraction (12). The authors concluded that the decrease in EMG activity of the MG at pronounced knee flexed positions is due to a critical force–length potential of all three muscles of the triceps surae (12).

The force produced by contracting muscle fibers is transmitted to bones via two passive structures: the aponeurosis and the tendon. These tendinous tissues play an important role as series-elastic-components and can store elastic energy during the movement (3). The VE-PC technique showed that the strain was heterogeneous with both the deep and superficial aponeurosis exhibiting positive and negative strains along the muscle length (3). The authors hypothesized that the observed aponeuroses strain may be linked to the distribution and orientation of the forces generated by the muscle fibers (3). The heterogeneity of fiber length and pennation angle in the proximo- distal direction of the MG may cause nonuniformity of fiber shortening with corresponding changes in regional aponeurosis strain. It is thus likely that, since varying the ankle angle leads to different muscle fiber architecture, it will not only affect muscle fiber strain but also the associated aponeuroses strains. Earlier studies focused on EMG activity and fiber lengths in the MG at rest and during activity at different knee flexion and ankle angles but did not measure muscle fiber and aponeurosis strain at varying ankle angles. Phase-contrast MR imaging has been successfully implemented to study muscle kinematics under different contraction paradigms (3, 4). The method is ideally suited to the measurement of muscle fiber and aponeurosis strains. The current study focuses on determining the strain in the MG muscle fiber and in the deep and superficial aponeuroses at different ankle angles and with different loads. Dynamic images of the

calf muscle were acquired with the foot positioned at plantarflexed, neutral, and dorsiflexed ankle angles and at two different loads corresponding to 25% and 50% of maximum voluntary contraction (MVC), with MVC determined at each foot position. Further, earlier work using dynamic MRI identified the muscle fiber direction by the fascicles on water suppressed images (4). However, especially in younger subjects, the fascicles are not always visualized consistently. The current paper explores an alternate way to extract regional muscle fiber direction using diffusion tensor imaging (DTI) without the additional complexity of fiber tractography. The hypotheses are (i) that MG fiber strain will be lowest in the dorsiflexed ankle position while producing the largest force at this ankle angle, (ii) fiber strains will deviate the most from linearity with %MVC in the plantarflexed position, and (iii) MG aponeurosis strain patterns will vary with the ankle angle reflecting the influence of fiber architecture.

METHODS

Subjects

The study was approved by the [redacted] and conformed to the standards in the Declaration of Helsinki on the use of human subjects in research. All subjects were included in this study after obtaining informed consent. Six healthy, moderately active, male subjects were examined in this study: (33.2 ± 16.3 yrs, height: 172.5 ± 7.0 cm, mass: 73.3 ± 6.5 kg).

MR Imaging

MR imaging was performed on a 1.5 Tesla Signa HDx MR scanner (GE Medical Systems, Milwaukee, WI) with an 8-Ch cardiac coil. Imaging was performed with the subject lying supine, feet first, with the dominant leg secured in a foot pedal fixture. The fixture allowed for the foot to

be positioned at three nominal ankle angles: dorsiflexion (***D***) 5˚, neutral (***N***) -25˚, and plantarflexion (***P***) -40˚. A large FOV image that included the ankle was collected at each foot position using the body coil to verify/estimate the ankle angle as well as to calculate the Achilles tendon moment arm. High-resolution water saturated fast-spin echo (echo time (TE): 12.9 ms, repetition time (TR): 925 ms, signal averages (NEX): 4, flip angle (FA): 20º, slice thickness/gap: 3/0 mm, field of view FA: 30 × 22.5 cm^2, matrix: 512 × 384) oblique sagittal slices of the calf muscle were collected where water signal is suppressed while the fascicles (fat) appear hyperintense. The slice with greatest fascicle visibility was selected for Velocity-Encoded Phase Contrast (VE-PC) imaging.

The dynamic gated VE-PC images were collected for a single oblique sagittal slice (TE: 7.7 ms, TR: 16.4 ms, signal averages (NEX): 2, flip angle (FA): 20º, slice thickness: 5 mm, field of view FA: 30 × 22.5 cm, partial-phase FOV: 0.55, matrix: 256 × 192, gated 22 phases, 3-direction velocity encoding with venc: 10 cm/s, 53 repetitions [192 (phase encode lines) × 0.55 (partial FOV) × 2 (NEX) / 4 (views per segment) = 53]) of 3 second isometric contraction cycles with total scan time 2 min and 39 sec. Force exerted by the subject during isometric contraction was detected by a strain sensor embedded in the foot-plate. Subjects were provided real-time visual feedback of the force generated superposed on the target force curve to facilitate consistent contractions. The differentiated force signal acted as the trigger for gated VE-PC image acquisition. Diffusion Tensor Imaging (DTI) images were acquired at anatomically and geometrically matched slices to the VE-PC image, using a SE-EPI DTI (TE/TR = 63 / 2200ms) sequence with 32 diffusion gradient directions, 3 slices. DTI images were acquired for each ankle angle and corrected for eddy

current artifacts, denoised (15), and processed for the eigenvalues/ eigenvectors and fractional anisotropy.

Force Measurements

The foot pedal's embedded strain sensor measurements were transmitted via optical fiber cable and recorded by a Data Acquisition device (National Instruments, TX, USA) connected to the computer. Maximum Voluntary Contraction (MVC) was measured for each subject at each ankle angle as the best of three trials recorded prior to imaging: $MVC_D = 271 \pm 49N$, $MVC_N = 140 \pm 29N$, $MVC_P = 66 \pm 20$ N (average over all 6 subjects). The MVCs were significantly different between the three ankle angles: $MVC_{D\text{-}N}$ ($p = 0.0012$), $MVC_{N\text{-}P}$ ($p = 0.0003$), and $MVC_{D\text{-}P}$ ($p = 0.0012$), where the subscripts are the two ankle angles compared in paired t-tests. VE-PC images were collected for submaximal contraction targets of 25% and 50% MVC. Torque was determined by multiplying the measured force values by the Achilles tendon moment arm (Figure 1).

Muscle Fiber Identification

The MG muscle on the VE-PC magnitude image was segmented into three regions corresponding to top third (proximal), middle third (middle) and lower third (distal) of its total length. Each region was eroded (3x3structuring element) to be well within the aponeurosis and filtered to remove all voxels with a Fractional Anisotropy less than 0.15 (to exclude noise, fat, and other non-contractile voxels). Since the DTI eigenvectors are 180° indeterminate, the lead eigenvector at each voxel was aligned to point in the same quadrant. The average of the lead eigenvector of each voxel in the region was computed. A line with the average in-plane direction of each region was placed in each

region's center; the ends of this line were extended to intersect the superficial and deep aponeurosis of the MG. This line was designated as the representative fiber direction for the region; a 'fiber direction' was identified for each of the three regions. It should be noted that the out-plane component of the lead DTI eigenvector was small, confirming the orientation of the oblique sagittal image captured the MG fibers in-plane of the slice. The DTI out-plane components of the lead DTI eigenvector averaged over the six subjects were small: 8.4%, 9.4% and 7.9% for dorsiflexion, neutral, and plantar flexion positions, respectfully.

Fiber Strains and Pennation angle

Phase-contrast images were corrected for phase shading artifacts and denoised using a 2D anisotropic diffusion filter (4). The endpoints of the DTI-identified muscle fibers were tracked through each frame of the dynamic study using the velocity data. Fiber angles were measured with respect to the y-axis of the image (SI direction). Changes in fiber angle were calculated from the initial angle of the fiber. Changes in fiber length were calculated with respect to the initial length and Lagrangian strains were computed. In addition, fiber strains normalized to force and torque were also computed. Strain, changes in fiber length and angle used in the statistical analysis were computed at the peak of the force curve.

Aponeurosis Analysis

The deep and superficial MG aponeuroses were manually identified on the first frame of the magnitude VE-PC image for each subject. Each aponeurosis was divided into 11 equal length segments starting from the proximal end of the tibia to the distal end of the MG and tracked through the frames of the dynamic study (3). Care was taken to position the points in the signal bearing

region adjacent to the aponeurosis but not on the aponeurosis itself which has no signal intensity. Length and Lagrangian strains were calculated for each aponeurosis segment for all temporal frames for each ankle angle and %MVC.

Statistical Analyses

The outcome variables of the fiber analysis are: fiber strain, normalized fiber strain (to force and to torque), fiber length, and pennation angle in the rest and peak contraction frames. Normality of data was tested using both the Shapiro-Wilk test and visual inspection of Q-Q plots. Three-way repeated measures analysis of ANOVA showed that there were no significant differences with fiber location (in the three regions: proximal, middle and distal) in any parameter except in the pennation angle. The values were averaged for the three regions in order to decrease the number of independent variables. Fiber strain and normalized fiber strains were normally distributed and for these variables, changes between ankle angles, % MVC as well as potential interaction effects (ankle angle x %MVC), were assessed using two-way repeated measures ANOVAs and in case of significant ANOVA results for the factor 'ankle angles', Bonferroni-adjusted post-hoc analyses were performed. When interactions were present, simple main effects were also examined. Muscle fiber length and pennation angles at rest and peak contraction were not distributed normally, so non-parametric testing was used. For these four outcome variables, the related samples test with Friedman's 2-way ANOVA by ranks with corrections for multiple comparisons was performed for ankle angle. For all tests, the level of significance was set at $\alpha = 0.05$. Data are reported as mean (SD) for the variables that are normally distributed and as median (interquartile range, IQR) for those not normally distributed. The statistical analyses were carried out in MATLAB (version R2021a. The MathWorks Inc. Natick, MA).

RESULTS

Figure 1 shows the ankle angles and the measurements for the Achilles tendon moment arms determined from large FOV sagittal slices. Figure 2 shows the fibers identified by the average of the lead eigenvector method for the proximal, middle, and distal regions of the MG for each % MVC and ankle angle for one subject; the fibers are superposed on high-resolution water saturated fast-spin echo images. The orientation of the fibers is as expected for the MG and follows the direction of fascicles. Supporting Figure 1 shows the video of the fibers with the motion of the fiber end points tracked through the dynamic cycle for one subject for the two %MVCs and at the three ankle angles.

Figure 3 depicts the changes in fiber angle, length and strain as a function of the contraction cycle for one subject. Table 1a lists the mean and standard deviation (over all subjects) of MVC, MVC torque, peak force, peak torque, fiber strain, and normalized fiber strain for each foot position and % MVC. Table 1b lists the median and interquartile range (over all subjects) of fiber architecture (length and pennation angle) at rest and at peak contraction. The peak strain was significantly lower at the lower %MVC ($p = 0.002$) and while peak strain was the lowest in the dorsiflexed position, it was not significantly different from other two ankle angles. Further, fiber strain changed significantly between 25 and 50 %MVCs in the dorsiflexed ($p = 0.004$) and neutral ($p = 0.034$) positions but not in the plantarflexed position. As (ankle angle * force) interaction was significant, simple main effects are reported for strain normalized to force and to torque. At both 50%MVC and 25% MVC, strain normalized to force was significantly different between each pairwise combination of ankle angles. At 50%MVC the p-values were for D-N ($p = 0.022$), D-P

($p = 0.004$), N-P ($p = 0.012$) and corresponding values at 25%MVC were $p = 0.037$, 0.012, 0.016 respectively. The absolute value of the normalized strain was lowest at the dorsiflexed position at 50% MVC while the highest normalized strain was at the plantarflexed position at 25% MVC. Comparing the normalized strain at 50 and 25% MVC at each ankle angle showed that significant changes with %MVC was only seen in the P ankle position ($p = 0.029$). The absolute value of normalized strain at 25% MVC was significantly higher than at 50% MVC for the P ankle angle. Statistically significant differences similar to strain normalized to force were obtained for strain normalized to torque. Significant differences were seen in the resting fiber length between D-P ($p < 0.001$) and D-N ($p = 0.023$) and in resting pennation angle between D-P ($p = 0.029$) while a trend was observed in D-N ($p = 0.059$) and N-P ($p = 0.059$). Resting fiber length decreased and pennation angle increased going from D to P. Significant differences in fiber length at peak contraction were seen with force ($p < 0.001$) and with ankle angle: D-P ($p < 0.001$) and D-N ($p < 0.001$). Significant differences in pennation angle at peak contraction were seen with force ($p < 0.001$) and with ankle angle: D-N ($p = 0.029$) and D-P ($p < 0.001$). At peak contraction, fiber lengths decreased and pennation angles increased compared to corresponding values at rest.

Figure 4a shows, for one subject, the schematic of the locations of the 11 points placed along the MG deep and superficial aponeuroses and the line segments connecting them at rest and at peak contraction. Figure 4b is box plot of the aponeurosis strain (estimated at peak force) in the 11 segments for the two %MVC and the three ankle angles averaged over the six subjects. Analysis of the strain comparing corresponding segments revealed no significant differences between the three ankle angles. Across all three ankle angles, aponeurosis strain was high at the distal and proximal regions of the muscle length and lowest in the middle where it was close to zero strain.

The distal end of the deep aponeurosis showed small positive strains whereas the superficial aponeurosis revealed negative strains at the distal end. Further, for the superficial aponeurosis, the absolute value of strains at the distal segments were the highest among all the segments. The deep aponeurosis showed the highest negative strains in the proximal end, higher than strain values in the superficial aponeurosis. The motion of the segments along the aponeurosis during the contraction cycle is shown in Supporting Figure 2.

A tentative analysis of the sarcomere length was performed assuming that the dorsiflexion ankle position was closer to optimal sarcomere length for maximum force than the other two ankle positions. A sarcomere length of 1.9 μm was assumed for the dorsiflexion ankle position; the choice of this reference sarcomere length in the D position was made to approximately follow the changes in MVC determined experimentally when going from D to N to P. Assuming this sarcomere length for the D position and with the measured fiber length, the number of sarcomeres was computed. As the number of sarcomeres is not expected to change with ankle angle, the same sarcomere number was used to calculate the sarcomere length for each muscle fiber length at rest and at 50% MVC (Table 2). Figure 5 shows the sarcomere lengths at rest (black) and at 50%MVC (red) superposed on theoretical F-L relationship plotted from data in (16).

DISCUSSION

Prior work used fascicles that were manually identified on water saturated anatomical images and the end points of these manually identified fibers were tracked through the dynamic cycle using the VE-PC data (4). This method was limited in utility due to the difficulty of identifying fascicles especially in young subjects. The reason that fascicles have high contrast on water saturated images is the presence of fat adjacent to the fascicles; however, the fat layer is minimal in younger subjects

making it difficult to view the fascicles. The method proposed here to automatically identify fibers from DTI data is shown to be feasible. It should be noted that the proposed method does not involve muscle fiber tractography which would provide the most accurate estimate of the fiber length and pennation angles. However, accurate and robust fiber tracking requires DTI data with the highest SNR (single voxel accuracy of the lead eigenvector for fiber tracking). In contrast, the SNR requirements to accurately determine the average of the lead eigenvector in a ROI (27 pixels are higher) are lower (17). The proposed method thus allows for short DTI acquisition times since it uses average data over fairly large ROIs (> 27 pixels). It should also be noted that a DTI scan is acquired at each ankle angle, so minimizing the acquisition time for DTI is important to keep the scan session to a clinically reasonable time. The DTI scans also confirmed that the method for selecting the oblique sagittal slice yielded MG fibers in the plane of the image.

The significant changes in MVC with ankle angle position in isometric contractions seen in the current study have been reported in earlier studies (12). The dependence of the MG MVC on the ankle angle position is attributed to ankle dorsiflexion stretching the gastrocnemius and bringing it closer to its optimal length in the force-length curve, which contributes to knee flexion strength and knee joint stability, thereby enabling greater muscle force (12). In all ankle positions, as anticipated, fiber length decreased and pennation angle increased at peak contraction compared to the values at rest. The current study also confirms US studies that showed fiber lengths and pennation angles to be significantly different between ankle positions at rest. However, the current study also shows that significant changes in fiber length and pennation angle with ankle angle (between D-N and D-P) persisted at peak contraction contrary to US studies that found no significant differences in the fiber lengths and pennation angles at peak force (12). This may reflect

the fact that US studies were at 100% MVC whereas the current study was at submaximal isometric contractions (25 and 50% MVC).

EMG activity of the MG has been reported to decrease during MVC for knee flexed positions and ankle angles at the more plantarflexed position (12). The main mechanism postulated in Ref. 12 for decreasing EMG activity and impairment in neuromuscular transmission-propagation at short muscle lengths is a neural inhibition. This is hypothesized as being triggered as the muscle reaches a critical shortened length at which, due to the force-length relationship, the torque output cannot be increased even if the muscle is fully activated. The human control system gets feedback regarding the force potential due to the force-length relationship of all three muscles of the triceps surae and regulates their activity to increase the economy of maximal torque generation (12). In contrast to the decrease in EMG activity at the more knee flexed/ plantarflexed ankle positions (12), fiber strain is higher at the P ankle position compared to the D ankle position (while D ankle angle MVC was higher than P ankle angle MVC). This points to the fact that the MG is inefficient in producing force in the plantarflexed ankle position; i.e., despite a larger contraction (strain) at the plantarflexed ankle position the force produced is smaller. The fact that the MG did not show decreased strains at the P ankle angle when going from 25 to 50% MVC indicates that it has not yet reached actively insufficiency at the P ankle angles of +30º and submaximal isometric contraction used in the current study.

Fiber strains in the MG were lower (though it did not reach significance) in the D ankle position compared to the P and N position and significantly higher at 50% MVC than at 25% MVC in the D and N positions. The increased strain at higher %MVC in the D and N ankle positions is understandable as increased contraction is required to generate the higher forces. In contrast to D

and N, the observation that the P ankle position did not show significant change in fiber strain with %MVC may indicate that the MG may be approaching the critical length where further contraction becomes more difficult. It is surprising that the fiber strains are lower in the D ankle position since in this ankle position, higher force is generated. It would be expected that the higher force in the D ankle angle will be accompanied by larger strains; the implication of the lower strains is that the D ankle angle position is ideal for force generation in that even small contractions (strains) are sufficient to generate large forces. Normalized fiber strains (normalized to force and torque) showed significant differences with ankle positions at both force levels. In comparing ankle positions, the D ankle position showed significantly lower normalized strains at both %MVCs than the N and P ankle positions; highlighting the fact that the D ankle position is at the optimum position for force production followed by N and the least optimal for the P ankle position. Smaller strains (contractions) are required to generate the same force at the dorsiflexed position than in the other two positions. Further, the absolute value of the normalized fiber strain was significantly higher at 25 %MVC than at 50% %MVC for the plantarflexed position. The latter finding is a reflection of strain not increasing significantly with %MVC in the P ankle position. It is likely that compared to the D and N positions, the contribution of the soleus to the total force increases in the P ankle position at higher %MVCs. The finding of lower strain and lower normalized strains in the dorsiflexed position while generating a high force should be of interest in rehabilitation paradigms, in optimizing athletic performance, and in minimizing strain injuries (18).

In terms of the aponeurosis strains during isometric contraction, ultrasound studies showed that the superficial and deep aponeuroses of medial gastrocnemius (MG) are uniformly stretched along their lengths in opposite directions; the superficial aponeurosis is stretched distally, whereas the

deep aponeurosis is stretched proximally (19). However, a study by Kinugasa et al using the MR VE-PC technique revealed heterogeneous aponeurosis strain patterns: positive strain occurred at both ends (proximal and distal) of the deep aponeurosis and in the proximal region of the superficial aponeurosis while negative strain was observed in the middle region of the deep aponeurosis and in the distal region of the superficial aponeurosis (3). Similar patterns of aponeurosis heterogeneity are also seen in the current study as in the earlier MR paper (3) if it is noted that the proximal most position of the current study is the third segment of the earlier study by Kinugasa et al (the latter study started the segments at the distal end of the femur while the current study starts at the proximal end the tibia). Thus, the positive strain that was seen in the first two proximal segments of the deep and superficial aponeuroses in the earlier study is not seen in the current study. Contrary to the hypothesis, the strain patterns did not show significant differences between the three ankle positions.

The length of sarcomeres that are arranged in series within a striated muscle fiber is one of the most important determinants of muscle force (16). As the ankle angle changes, the fibers of the MG and their constituent sarcomeres change length, which shifts the sarcomeres' positions on the sarcomere force–length curve and affects the force-generating capacity of the muscle. It should be noted that the current study did not measure sarcomere length directly at any of the ankle angles but given the highest value of force at dorsiflexion position, this ankle position was assumed to closer to the optimum sarcomere length than the N or P positions. Further, as seen in the current study the sarcomere lengths of the MG at different ankle angles are positioned on the ascending limb of the F-L curve. This has also been observed in ultrasound and dynamometry studies of the soleus where it was shown that soleus acts on the ascending limb during active contractions (20).

It should be noted that the choice of the reference sarcomere length at 1.9 μm for the D position was dictated by considerations that the calculated sarcomere lengths at other ankle angles resulted in force decreases on the F-L curve close to that observed experimentally. Based on the F-L curve, the choice of the optimal sarcomere length of 2.65 μm severely underestimated the observed force decrease with ankle angle. In fact, even the reference value of 1.9 μm underestimates the force decreases with ankle angles. These results potentially indicate that there may be other determinants of the observed force changes with ankle angle beyond changes in the sarcomere length. As the aponeurosis strains are not different between the ankle angles, this is not likely to contribute to the observed force changes. It should also be noted that while an isometric contraction implies no change in muscle length, it does not mean imply an unchanged muscle fiber length. As seen experimentally, muscle fiber contracts and rotates leading to the points at peak contraction shifting further down the ascending limb of the F-L curve. It is possible that the force potential is determined by an average of the rest and peak sarcomere length than just the rest sarcomere length. It is also likely that factors other than changes in sarcomere length may contribute to the measured force changes. It is important to emphasize that the current method does not provide absolute values of sarcomere length but by mapping the force and fiber lengths at rest and at peak contraction as a function of ankle position, one can determine whether the sarcomere length is positioned on the descending or the ascending limb of the force-length curve. Muscle contractures that result from upper motor lesion in patients with cerebral palsy are often treated by surgical lengthening (21). It would be a great clinical tool to know prior to surgery if the patient's sarcomere length is on the ascending or descending limb of the FL curve (21, 22).

There are some limitations to the current study, the main one is the small sample size. However, it should be noted that the repeated measures ANOVA has higher statistical power since the variability in the subject population is taken into account. Further, statistically significant differences in fiber strain, normalized fiber strains and in fiber architecture with force and ankle angles were identified in the current small study. The study was in 2D while true muscle fibers traverse a 3Dal space both at rest and at the peak of the contraction. However, care was taken to position the oblique sagittal slice such that the fibers of the MG lay in the plane of the image; this was subsequently verified by the DTI based analysis which showed that the fibers ran predominantly in-plane.

In summary, the current paper focuses on muscle fiber and aponeurosis strains obtained at two levels of submaximal isometric contractions with the ankle angle varied from dorsiflexion to neutral to plantarflexed. The dorsiflexed ankle position generated significantly greater force while exhibiting significantly lower normalized strains than the neutral or plantarflexed position. The sarcomere lengths at rest and at peak force were calculated assuming a reference optimal sarcomere length at the dorsiflexed ankle angle and the MG was identified to be working in the ascending limb of the FL curve. The analysis of the sarcomere lengths and their relative positions on the F-L curve also revealed that there may be other determinants to force changes with ankle position in addition to changes in sarcomere length.

REFERENCES

1. Karakuzu A, Pamuk U, Ozturk C, Acar B, Yucesoy CA: Magnetic resonance and diffusion tensor imaging analyses indicate heterogeneous strains along human medial gastrocnemius fascicles caused by submaximal plantar-flexion activity. *J Biomech.* 2017; 57:69-78.
2. Pamuk U, Karakuzu A, Ozturk C, Acar B, Yucesoy CA: Combined magnetic resonance and diffusion tensor imaging analyses provide a powerful tool for in vivo assessment of deformation along human muscle fibers. *J Mech Behav Biomed Mater.* 2016; 63:207-219.
3. Kinugasa R, Shin D, Yamauchi J, et al.: Phase-contrast MRI reveals mechanical behavior of superficial and deep aponeuroses in human medial gastrocnemius during isometric contraction. *J Appl Physiol* 2008; 105:1312–1320.
4. Sinha U, Malis V, Csapo R, Moghadasi A, Kinugasa R, Sinha S. Age-related differences in strain rate tensor of the medial gastrocnemius muscle during passive plantarflexion and active isometric contraction using velocity encoded MR imaging: potential index of lateral force transmission. *Magn Reson Med* 2015; 73:1852–63.
5. Moo EK, Leonard TR, Herzog W: The sarcomere force-length relationship in an intact muscle-tendon unit. *Journal of Experimental Biology* 2020; 223: jeb215020.
6. Gordon AM, Huxley AF, Julian FJ: The variation in isometric tension with sarcomere length in vertebrate muscle fibres. *J Physiol* 1966; 184:170–192.
7. Maganaris CN: Force-length characteristics of in vivo human skeletal muscle. *Acta Physiol Scand* 2001; 172:279–285.
8. Kim K, Cha Y-J, Fell DW: Differential effects of ankle position on isokinetic knee extensor and flexor strength gains during strength training. *Isokinet Exerc Sci* 2016; 24:195–199.

9. Lee JWY, Mok K-M, Chan HCK, Yung PSH, Chan K-M: Eccentric hamstring strength deficit and poor hamstring-to-quadriceps ratio are risk factors for hamstring strain injury in football: A prospective study of 146 professional players. *J Sci Med Sport* 2018; 21:789–793.
10. Panoutsakopoulos V, Kotzamanidou MC, Papaiakovou G, Kollias IA: The Ankle Joint Range of Motion and Its Effect on Squat Jump Performance with and without Arm Swing in Adolescent Female Volleyball Players. *J Funct Morphol Kinesiol* 2021; 6:14.
11. Maganaris CN: Force-length characteristics of the in vivo human gastrocnemius muscle. *Clin Anat* 2003; 16:215–223.
12. Arampatzis A, Karamanidis K, Stafilidis S, Morey-Klapsing G, DeMonte G, Brüggemann G-P: Effect of different ankle- and knee-joint positions on gastrocnemius medialis fascicle length and EMG activity during isometric plantar flexion. *Journal of Biomechanics* 2006:1891–1902.
13. Wakahara T, Kanehisa H, Kawakami Y, Fukunaga T: Fascicle behavior of medial gastrocnemius muscle in extended and flexed knee positions. *J Biomech* 2007; 40:2291–2298.
14. Wakahara T, Kanehisa H, Kawakami Y, Fukunaga T: Effects of knee joint angle on the fascicle behavior of the gastrocnemius muscle during eccentric plantar flexions. *J Electromyogr Kinesiol* 2009; 19:980–987.
15. Tristán-Vega A, Aja-Fernández S. Joint LMMSE estimation of DWI data for DTI processing. *Med Image Comput Comput Assist Interv* 2008; 11:27–34.
16. Lichtwark GA, Farris DJ, Chen X, Hodges PW, Delp SL: Microendoscopy reveals positive correlation in multiscale length changes and variable sarcomere lengths across different regions of human muscle. *J Appl Physiol* 2018; 125:1812–1820.
17. Damon BM: Effects of image noise in muscle diffusion tensor (DT)-MRI assessed using numerical simulations. *Magnetic Resonance in Medicine* 2008:934–944.

18. Rehorn MR, Blemker SS: The effects of aponeurosis geometry on strain injury susceptibility explored with a 3D muscle model. *J Biomech* 2010; 43:2574–2581.
19. Muramatsu T, Muraoka T, Kawakami Y, Fukunaga T: Superficial aponeurosis of human gastrocnemius is elongated during contraction: implications for modeling muscle-tendon unit. J Biomech 2002; 35:217–223.
20. Rubenson J, Pires NJ, Loi HO, Pinniger GJ, Shannon DG: On the ascent: the soleus operating length is conserved to the ascending limb of the force-length curve across gait mechanics in humans. *Journal of Experimental Biology* 2012.
21. Mathewson MA, Ward SR, Chambers HG, Lieber RL: High resolution muscle measurements provide insights into equinus contractures in patients with cerebral palsy. *J Orthop Res* 2015; 33:33–39.
22. Mathewson MA, Lieber RL: Pathophysiology of muscle contractures in cerebral palsy. *Phys Med Rehabil Clin N Am* 2015; 26:57–67.

TABLES

Table 1a: Muscle fiber strain and fiber strain normalized to force and to torque.

Ankle Position	% MVC	MVC (N)	MVC Torque (Nm)	Peak Force (N)	Peak Torque (Nm)	[1d] Peak Strain	[1a, 1b, 1c, 1d, 2a, 2b, 2c, 2d] Strain / Force (1/N)	[1a, 1b, 1c, 1d, 2a, 2b, 2c, 2d] Strain / Torque (1/Nm)
D	50%	271.0 [48.7]	13.0 [3.9]	131.0 [31.1]	6.2 [2.0]	-0.1545 [0.0656]	-0.0013 [0.0007]	-0.0278 [0.0160]
D	25%	271.0 [48.7]	13.0 [3.9]	68.5 [15.7]	3.3 [1.0]	-0.1029 [0.0466]	-0.0015 [0.0007]	-0.0333 [0.0155]
N	50%	140.2 [29.2]	6.9 [0.6]	71.9 [20.1]	3.5 [0.6]	-0.2179 [0.0945]	-0.0032 [0.0016]	-0.0647 [0.0336]
N	25%	140.2 [29.2]	6.9 [0.6]	36.2 [10.4]	1.8 [0.3]	-0.1539 [0.0774]	-0.0045 [0.0025]	-0.0898 [0.0517]
P	50%	66.4 [20.5]	3.2 [0.7]	31.6 [13.9]	1.5 [0.7]	-0.2084 [0.0730]	-0.0076 [0.0036]	-0.1555 [0.0699]
P	25%	66.4 [20.5]	3.2 [0.7]	16.4 [7.4]	0.8 [0.4]	-0.1742 [0.0694]	-0.0123 [0.0061]	-0.2570 [0.1319]

Note: Ankle positions are dorsiflexion (D), neutral (N), and plantar flexion (P).
Standard deviation values are provided in square brackets beneath mean values.

[1a] 50% MVC: Significant difference between ankle positions D and N
[1b] 50% MVC: Significant difference between ankle positions N and P
[1c] 50% MVC: Significant difference between ankle positions D and P
[1d] D and N: Significant difference between 25% and 50% MVC
[2a] 25% MVC: Significant difference between ankle positions D and N
[2b] 25% MVC: Significant difference between ankle positions N and P
[2c] 25% MVC: Significant difference between ankle positions D and P
[2d] P ankle angle: Significant difference between 25% and 50% MVC

Table 1b: Muscle fiber architecture at rest and at peak contraction.

Ankle Position	% MVC	[c] Rest Angle (°)	[a, c, d] Peak Contr.* Angle (°)	[a, c] Rest Length (mm)	[a, c, d] Peak Contr.* Length (mm)
D	50%	32.2 [1.5]	34.1 [3.3]	42.6 [13.6]	35.9 [11.4]
D	25%	32.2 [1.5]	33.4 [4.6]	42.6 [13.6]	38.8 [13.0]
N	50%	33.3 [3.5]	34.6 [7.3]	34.5 [11.8]	28.2 [10.7]
N	25%	33.3 [3.5]	33.2 [5.3]	34.5 [11.8]	32.0 [13.8]
P	50%	35.1 [4.3]	37.3 [5.7]	29.0 [5.8]	23.0 [6.2]
P	25%	35.1 [4.3]	36.6 [5.6]	29.0 [5.8]	25.2 [5.2]

Note: Ankle positions are dorsiflexion (D), neutral (N), and plantar flexion (P).
Interquartile range is provided in square brackets beneath median values.
*Contr.: abbreviation for contraction.
[a] significant difference between ankle positions D and N.
[b] significant difference between ankle positions N and P.
[c] significant difference between ankle positions D and P.
[d] significant difference between 25% and 50% of maximum voluntary contraction (MVC).

Table 2: Muscle fiber length and sarcomere length at rest and at peak contraction.

Ankle Position	Number of Sarcomeres	Rest Sarcomere Length (μm)	Rest Fiber Length (mm)	Peak Contr.* Sarcomere Length (μm)	Peak Contr.* Fiber Length (mm)
D	24526	1.9	46.6	1.6	39.8
N	24526	1.5	37.6	1.2	29.9
P	24526	1.4	33.2	1.1	26.6

Note: Ankle positions are dorsiflexion (D), neutral (N), and plantar flexion (P).
*Contr.: abbreviation for contraction.

FIGURE LEGENDS

Figure 1: Large field of view (FOV) images for one subject at the three ankle angles (left: dorsiflexed, middle: neutral, right: plantarflexed ankle positions). The images document the actual ankle angle as shown here in the angle measurements at each ankle position. In addition, the Achilles tendon moment arm was determined in these images as the perpendicular distance between the identified Achilles tendon (between points labeled '1' and '2') and the center of the ankle (point '3').

Figure 2: The fibers identified by the proposed method using the DTI lead eigenvector data are shown in green dashed lines in the three regions of the muscle (proximal, middle and distal) superposed on the water saturated Fast Spin Echo images (muscle appears dark while the fascicles due to the presence of fat appear bright on these images). A few fascicles in the MG can be seen on the water saturated images and these are approximately aligned with the DTI derived fibers (identified by green arrows). It can be seen that not many fascicles are visible in the MG while the proposed technique using DTI is effective in identifying the muscle fibers.

Figure 3: The variation, as a function of the dynamic cycle, of change in fiber angle from the initial frame, change in fiber length from the initial frame and fiber strain is shown for one subject (top row: dorsiflexed (D) ankle position, middle row: neutral (N) ankle position, bottom row: plantarflexed (P) ankle position. The changes with %MVC is the least for the plantarflexed position. The values at the peak of the contraction are reported in Tables 1a and 1b (averaged over the six subjects).

Figure 4a: The end points of the 11 segments are shown for the medial gastrocnemius deep (green) and superficial (blue) aponeuroses. The points on the soleus to track the aponeurosis are shown in red. The top row shows at 50% MVC while the bottom row is at 25% MVC. The schematic is presented in pairs (at rest and at peak contractions) from left to right: dorsiflexed (D), neutral (N), plantarflexed (P) ankle angles. In the paired schematics, the segments at the moment of peak contraction are shown as shortening (thick solid line), expanding (dotted line) or unchanged (thin solid line).

Figure 4b: Plot of the segmental strain values extracted at peak of the dynamic contraction for 50% MVC (top row) and for 25% MVC (bottom row) for dorsiflexion (D), Neutral (N) and plantarflexion (P) ankle angle positions. Segment 1 is the proximal end while segment 11 is the distal end of the aponeuroses, the segments are arranged vertically starting from distal (lower end) to proximal end (top) so that it aligns with the segments shown in Fig. 4a. Each segment has three bar plots corresponding to red (Soleus), green (deep aponeurosis), blue (superficial aponeurosis); there are eleven sets with three bar plots each corresponding to the eleven segments in Fig. 4a. The close match of the segments tracked from the soleus and medial gastrocnemius sides of the distal aponeurosis (red and green, respectively) is a check of the internal consistency of the velocity-based tracking.

Figure 5: The Force- Length curve (solid line) is plotted based on data from Ref. 18. The black markers pertain to the sarcomere length calculated for the resting fiber length at each ankle angle (Dorsiflexion: D, Neutral: N, Plantar flexion: P) while the red markers are calculations made with lengths at peak contraction at 50% MVC (Table 2). All values were calculated using

average values of fiber lengths for the six subjects. An initial estimate of 1.9 microns for the dorsiflexed position was made to approximately follow the experimentally observed changes in force with ankle angle.

Supporting Figure 1: Fibers (white lines) identified from the DTI images shown superposed on the magnitude images of the velocity encoded phase contrast sequence. Cine images of the fibers tracked through the dynamic cycle are shown for one subject. Fiber end points are tracked from the initial to the final frame using the voxel level velocity data. The top row shows cine images at 50% MVC and the bottom row at 25% MVC. The columns are from left to right: dorsiflexed (D), neutral (N) and plantarflexed (P) ankle positions.

Supporting Figure 2: Cine images of the aponeurosis segments (MG distal and superficial) tracked through the dynamic cycle are shown for one subject. The MG deep aponeurosis is also tracked from the soleus side. Segment end points are tracked from the initial to the final frame using the voxel level velocity data. The top row shows cine images at 50% MVC and the bottom row at 25% MVC. The columns are from left to right: dorsiflexed (D), neutral (N), and plantarflexed (P) ankle positions. The segments from the soleus and medial gastrocnemius sides of the distal aponeurosis closely track each other, confirming the validity of the technique.

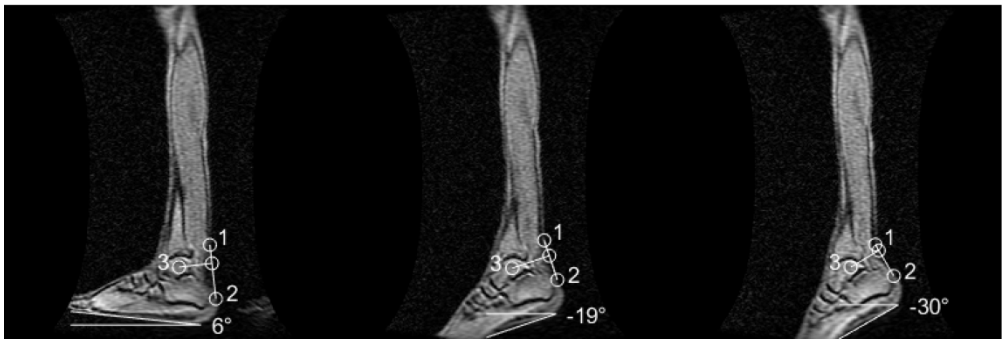

Figure 1: Large field of view (FOV) images for one subject at the three ankle angles (left: dorsiflexed, middle: neutral, right: plantarflexed ankle positions). The images document the actual ankle angle as shown here in the angle measurements at each ankle position. In addition, the Achilles tendon moment arm was determined in these images as the perpendicular distance between the identified Achilles tendon (between points labeled '1' and '2') and the center of the ankle (point '3').

325x108mm (300 x 300 DPI)

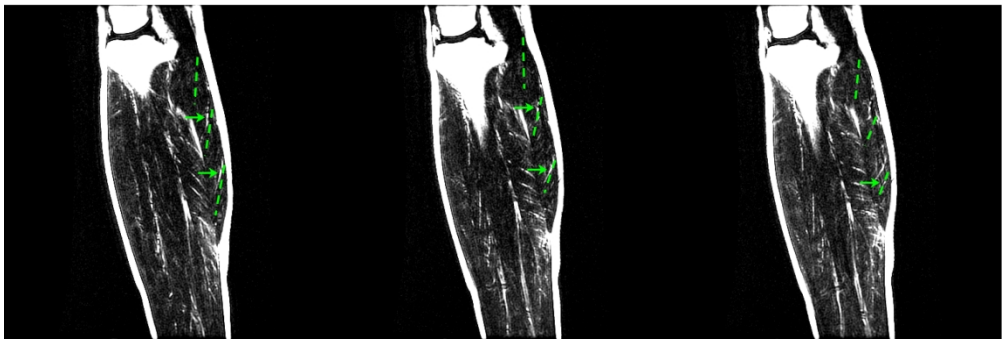

Figure 2: The fibers identified by the proposed method using the DTI lead eigenvector data are shown in green dashed lines in the three regions of the muscle (proximal, middle and distal) superposed on the water saturated Fast Spin Echo images (muscle appears dark while the fascicles due to the presence of fat appear bright on these images). A few fascicles in the MG can be seen on the water saturated images and these are approximately aligned with the DTI derived fibers (identified by green arrows). It can be seen that not many fascicles are visible in the MG while the proposed technique using DTI is effective in identifying the muscle fibers.

325x108mm (300 x 300 DPI)

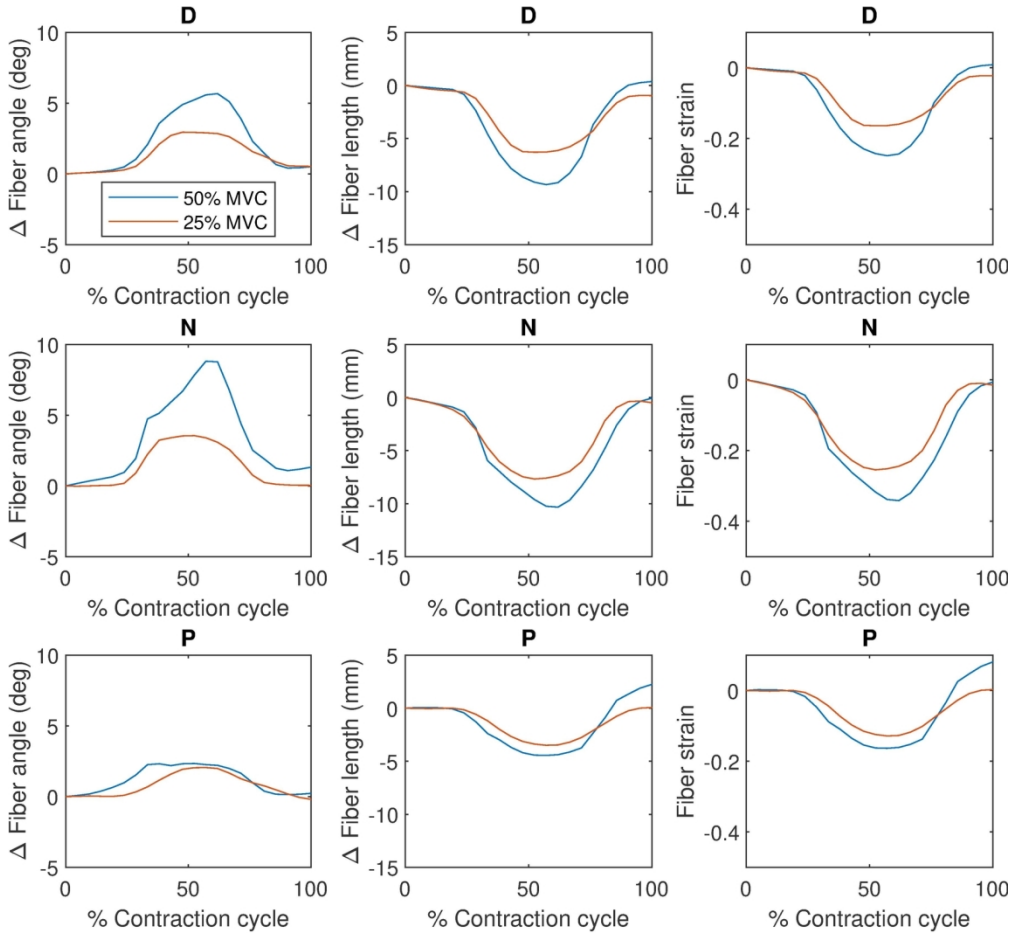

Figure 3: The variation, as a function of the dynamic cycle, of change in fiber angle from the initial frame, change in fiber length from the initial frame and fiber strain is shown for one subject (top row: dorsiflexed (D) ankle position, middle row: neutral (N) ankle position, bottom row: plantarflexed (P) ankle position. The changes with %MVC is the least for the plantarflexed position. The values at the peak of the contraction are reported in Tables 1a and 1b (averaged over the six subjects).

152x141mm (300 x 300 DPI)

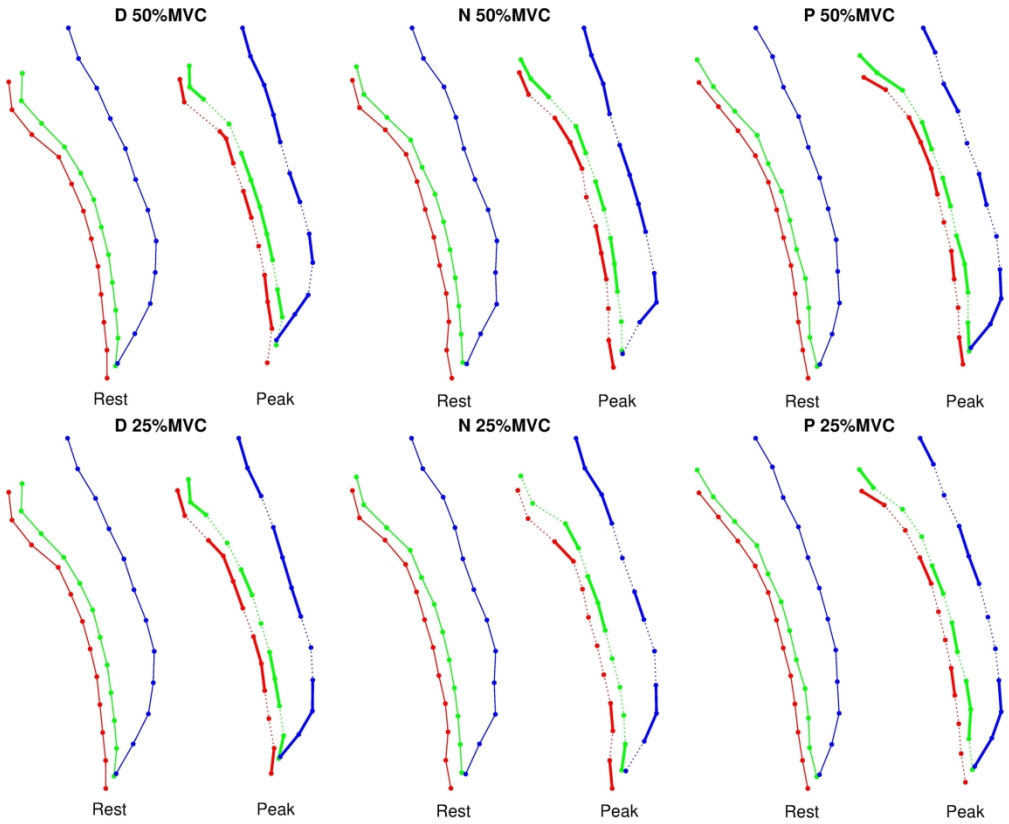

Figure 4a: The end points of the 11 segments are shown for the medial gastrocnemius deep (green) and superficial (blue) aponeuroses. The points on the soleus to track the aponeurosis are shown in red. The top row shows at 50% MVC while the bottom row is at 25% MVC. The schematic is presented in pairs (at rest and at peak contractions) from left to right: dorsiflexed (D), neutral (N), plantarflexed (P) ankle angles. In the paired schematics, the segments at the moment of peak contraction are shown as shortening (thick solid line), expanding (dotted line) or unchanged (thin solid line).

208x168mm (300 x 300 DPI)

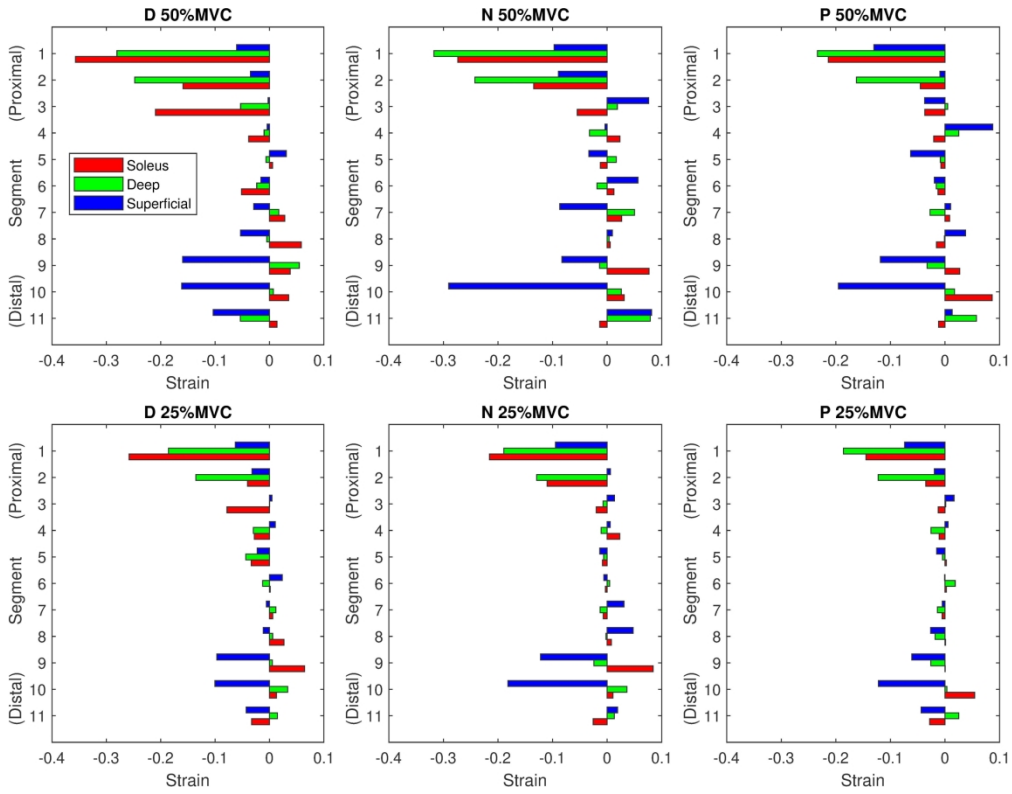

Figure 4b: Plot of the segmental strain values extracted at peak of the dynamic contraction for 50% MVC (top row) and for 25% MVC (bottom row) for dorsiflexion (D), Neutral (N) and plantarflexion (P) ankle angle positions. Segment 1 is the proximal end while segment 11 is the distal end of the aponeuroses, the segments are arranged vertically starting from distal (lower end) to proximal end (top) so that it aligns with the segments shown in Fig. 4a. Each segment has three bar plots corresponding to red (Soleus), green (deep aponeurosis), blue (superficial aponeurosis); there are eleven sets with three bar plots each corresponding to the eleven segments in Fig. 4a. The close match of the segments tracked from the soleus and medial gastrocnemius sides of the distal aponeurosis (red and green, respectively) is a check of the internal consistency of the velocity-based tracking.

218x169mm (300 x 300 DPI)

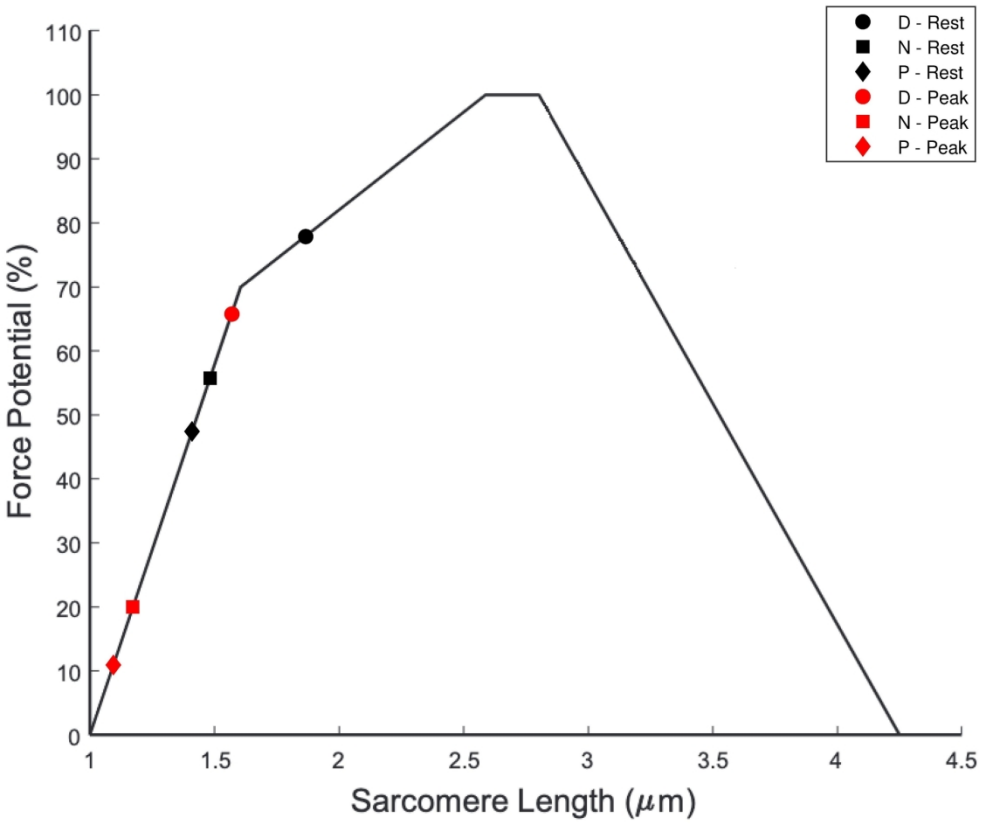

Figure 5: The Force- Length curve (solid line) is plotted based on data from Ref. 18. The black markers pertain to the sarcomere length calculated for the resting fiber length at each ankle angle (Dorsiflexion: D, Neutral: N, Plantar flexion: P) while the red markers are calculations made with lengths at peak contraction at 50% MVC (Table 2). All values were calculated using average values of fiber lengths for the six subjects. An initial estimate of 1.9 microns for the dorsiflexed position was made to approximately follow the experimentally observed changes in force with ankle angle.

174x147mm (300 x 300 DPI)